Inorg. Chem. **2007**, *46*, 4530–4534

A Heterometallic Porous Material for Hydrogen Adsorption

Ying Wang, Peng Cheng,* Jun Chen, Dai-Zheng Liao, and Shi-Ping Yan

Department of Chemistry, Nankai University, Tianjin 300071, P. R. China

Received January 19, 2007

Two kinds of heterometallic complexes, $\{[Sm_2(L)_6Co_2][Co(H_2O)_6]\cdot 3H_2O\}_n$ (**Sm**–**Co**) and $\{[Sm_2(L)_6Zn_3(H_2O)_6]\cdot 1.5H_2O\}_n$ (**Sm**–**Zn**) (H_2L = oxydiacetic acid), were synthesized under hydrothermal conditions. In **Sm**–**Co**, each L chelates to one Sm^{3+} center and bonds to two Co^{2+} ions in an *anti-anti* configuration. Sm and Co atoms are arrayed alternatively and connected by O–C–O bridges to form a cubic octahedral cage as the secondary building unit. Consequently, topological NaCl nets with high symmetry in the cubic space group $Fd\bar{3}c$ have been constructed. It is interesting to note that **Sm**–**Co** contains interesting 2-fold interpenetrating 3D hydrogen-bonding supramolecular networks while in **Sm**–**Zn** each L adopts a *syn-syn* configuration to link two Zn^{2+} ions. Carboxylate groups bridge adjacent Sm and Zn atoms to create two kinds of metallocycles, $Sm_2(COO)_4Zn_2$ and $Sm_6(COO)_{12}Zn_6$, to be further assembled into a highly ordered 3D nanotubular structure. **Sm**–**Zn** represents the largest porous material among the heterometallic coordination polymers and the first example in the investigation of hydrogen adsorption. **Sm**–**Zn** possesses hydrogen storage capacity of up to 1.19 wt % at 77 K and 0.54 wt % at 298 K, respectively.

Introduction

Porous materials can offer considerable internal surface area for separation, manipulation, and catalytic transformation of guest molecules, which may be proposed for gas storage.[1] The desire for exploitation of new materials with high-capacity hydrogen storage is a present day challenge for the real use of hydrogen as a fuel, promoted by industrial and environmental applications.[2−5] Many compounds are able to store large amounts of hydrogen depending on two different mechanism, chemisorption or physisorption. Due to low density and large surface area and void volume, one of the most interesting classes of porous materials comprising the open metal−organic frameworks (MOFs) has recently emerged as promising adsorbents for hydrogen storage during the physisorption process. However, little data are available for their sorption behavior at saturation,[6] a criteria taken into account in the design of new hybrid solids showing improved hydrogen-storage properties. Up to now, the design and synthesis of such materials have been almost centered on monometallic 3D MOFs. Heterometallic porous coordination polymers, especially containing rare-earth ions, have received much less attention,[7] due to the variable and versatile coordination behavior of 4f-metal ions.

Encouraged by our recent success in exploiting functional 3d−4f coordination polymers based on pyridine-2,6-dicarboxylic acid (H_2dipic),[7a,8] we turned to a flexible ligand oxydiacetic acid (H_2L)[9] as the molecular building block.

* To whom correspondence should be addressed. E-mail: pcheng@nankai.edu.cn.

(1) See for selected recent reviews: (a) Kitagawa, S.; Kitaura, R.; Noro, S. *Angew. Chem., Int. Ed.* **2004**, *43*, 2334. (b) Férey, G.; Mellot-Draznieks, C.; Serre, C.; Millange, F. *Acc. Chem. Res.* **2005**, *38*, 217. (c) Bradshaw, D.; Claridge, J. B.; Cussen, E. J.; Prior, T. J.; Rosseinsky, M. J. *Acc. Chem. Res.* **2005**, *38*, 273. (d) Fujita, M. *Acc. Chem. Res.* **1999**, *32*, 53. (e) Dincã, M.; Dailly, A.; Liu, Y.; Brown, C. M.; Neumann, D. A.; Long, J. R. *J. Am. Chem. Soc.* **2006**, *128*, 16876. (f) Eddaoudi, M.; Moler, D. B.; Li, H. L.; Chen, B. L.; Reineke, T. M.; O'Keeffe, M.; Yaghi, O. M. *Acc. Chem. Res.* **2001**, *34*, 319.

(2) (a) Pan, L.; Parker, B.; Huang, X. Y.; Olson, D. H.; Lee, J. Y.; Li, J. *J. Am. Chem. Soc.* **2006**, *128*, 4180. (b) Rowsell, J. L. C.; Spencer, E. C.; Eckert, J.; Howard, J. A. K.; Yaghi, O. M. *Science* **2005**, *309*, 1350.

(3) (a) Latroche, M.; Surblé, S.; Serre, C.; Mellot-Draznieks, C.; Llewellyn, P. L.; Lee, J.; Chang, J.-S.; Jhung, S. H.; Férey, G. *Angew. Chem., Int. Ed.* **2007**, *46*, 8227 and references cited therein. (b) Bradshaw, D.; Prior, T. J.; Cussen, E. J.; Claridge, J. B.; Rosseinsky, M. J. *J. Am. Chem. Soc.* **2004**, *126*, 6106. (c) Millward, A. R.; Yaghi, O. M. *J. Am. Chem. Soc.* **2005**, *127*, 17998.

(4) (a) Dincã, M.; Long, J. R. *J. Am. Chem. Soc.* **2005**, *127*, 9376. (b) Sun, D.; Ma, S.; Ke, Y.; Collins, D. J.; Zhou, H.-C. *J. Am. Chem. Soc.* **2006**, *128*, 3896. (c) Dietzel, P. D. C.; Panella, B.; Hirscher, M.; Blom, R.; Fjellväg, H. *Chem. Commun.* **2006**, 959.

(5) (a) Humphrey, S. M.; Chang, J.-S.; Jhung, S. H.; Yoon, J. W.; Wood, P. T. *Angew. Chem., Int. Ed.* **2007**, *46*, 272 and references cited therein. (b) Rowsell, J. L. C.; Yaghi, O. M. *Angew. Chem., Int. Ed.* **2005**, *44*, 4670.

(6) Wong-Foy, A. G.; Matzger, A. J.; Yaghi, O. M. *J. Am. Chem. Soc.* **2006**, *128*, 3494.

(7) (a) Zhao, B.; Cheng, P.; Dai, Y.; Cheng, C.; Liao, D.-Z.; Yan, S.-P.; Jiang, Z.-H.; Wang, G.-L. *Angew. Chem., Int. Ed.* **2003**, *42*, 934. (b) Ren, Y.-P.; Long, L.-S.; Mao, B.-W.; Yuan, Y.-Z.; Huang, R.-B.; Zheng, L.-S. *Angew. Chem., Int. Ed.* **2003**, *42*, 532. (c) Imaz, I.; Bravic, G.; Sutter, J.-P. *Chem. Commun.* **2005**, 993.

10.1021/ic070097r CCC: $37.00
Published on Web 04/26/2007

Since oxydiacetic acid has coordination sites similar to those of H_2dipic to link both 3d and 4f metals, we surmised that new heterometallic porous materials with nanometer-scale voids should be yielded by the reaction of H_2L with divalent metal ions and Ln(III) ions.

Here, we report the syntheses and crystal structures of $\{[Sm_2(L)_6Co_2][Co(H_2O)_6]\cdot 3H_2O\}_n$ (**Sm−Co**) and $\{[Sm_2(L)_6Zn_3(H_2O)_6]\cdot 1.5H_2O\}_n$ (**Sm−Zn**). Different ligand configurations, the major driving force to produce two types of products, result in different assembly directions of Sm^{3+} and transition metal ions. **Sm−Co** represents a kind of anionic porous MOF, which is rare in 3D zeolite-like coordination polymers and contains 2-fold interpenetrating 3D hydrogen-bonding supramolecular network, while **Sm−Zn** represents the largest porous material among the heterometallic coordination polymers and the first example for the investigation of hydrogen adsorption.

Experimental Section

Materials. All reagents and solvents were commercially available and used as received without further purification. Analyses for C, H, and N were carried out on a Perkin-Elmer analyzer. TGA experiments were performed on a NETZSCH TG 209 instrument with a heating rate of 10 °C min^{-1}. Powder X-ray diffraction measurements were recorded on a D/Max-2500 X-ray diffractometer using Cu Kα radiation. The pressure−composition−temperature (P−C−T) curves for hydrogen adsorption were determined by using a computer-controlled "gas reaction controller" apparatus, which was manufactured by the Advanced Materials Corp. (AMC, Pittsburgh, PA, http://www.advancedmaterial.com). The microcrystal samples of **Sm−Zn**, typically 500 mg in weight, were placed into a stainless steel vacuum system. The volume in the hydrogen adsorption process had been carefully calibrated before the actual measurement. The hydrogen adsorption was carried out at temperatures of 77 and 298 K and under hydrogen pressures ranging from 1.3×10^{-5} to 3.5 MP. Ultrahigh-purity hydrogen (99.999%) was used. The hydrogen adsorption amount was defined as the ratio of the mass gain and the mass of the starting **Sm−Zn** plus adsorbed hydrogen. The surface area and micropore volume of **Sm−Zn** were performed at the Tianjin Research & Design Institute of Chemical Industry with a Quantachrome instrument.

Table 1. Crystallographic Data and Details of Refinements for **Sm−Co** and **Sm−Zn**

param	Sm−Co	Sm−Zn
empirical formula	$C_{12}H_{21}O_{19.5}SmCo_{1.5}$	$C_{12}H_{19.5}O_{18.75}SmZn_{1.5}$
M_r	716.03	712.18
cryst system	cubic	hexagonal
space group	$Fd\bar{3}c$	$P6/mcc$
a/Å	25.9723(6)	14.8127(14)
b/Å	25.9723(6)	14.8127(14)
c/Å	25.9723(6)	15.613(3)
α/deg	90	90
β/deg	90	90
γ/deg	90	120
V/Å^3	17519.9(7)	2966.7(7)
Z	32	4
cryst size/mm	0.22 × 0.14 × 0.12	0.20 × 0.16 × 0.12
D_c/g cm^{-3}	2.172	1.595
μ/mm^{-1}	3.872	3.229
F(000)	11 248	1394
θ range/deg	2.22−27.71	1.59−26.42
tot. data	25 210	15 254
unique data	865	1069
R_{int}	0.0334	0.0413
R1[a] [$I > 2\sigma(I)$]	0.0316	0.0408
wR2[a] [$I > 2\sigma(I)$]	0.0741	0.1273
S[b]	1.078	1.149

[a] $R1(F_o) = \sum||F_o| - |F_c||/|F_o|$, $wR2(F_o^2) = [\sum w(F_o^2 - F_c^2)^2/\sum w(F_o^2)^2]^{1/2}$. [b] $S = \{\sum[w(F_o^2 - F_c^2)^2]/(n - p)\}^{1/2}$.

Preparations. Synthesis of $\{[Sm_2(L)_6Co_2][Co(H_2O)_6]\cdot 3H_2O\}_n$ (Sm−Co) and $\{[Sm_2(L)_6Zn_3(H_2O)_6]\cdot 1.5H_2O\}_n$ (Sm−Zn). A mixture of Sm_2O_3 (0.1 mmol), $M(CH_3COO)_2$ (0.3 mmol, M = Co for **Sm−Co** and Zn for **Sm−Zn**), H_2L (0.6 mmol), and H_2O (12 mL) were put in a 20 mL acid digestion bomb and heated at 180 °C for 3 days. The crystal products were collected after washing with H_2O (2 × 5 mL) and diethyl ether (2 × 5 mL). Yield: 65% for **Sm−Co** and 70% for **Sm−Zn**, respectively, based on Sm_2O_3. Anal. Calcd for **Sm−Co** ($C_{12}H_{21}O_{19.5}SmCo_{1.5}$): C, 20.13; H, 2.96. Found: C, 20.38; H, 2.82. Calcd for **Sm−Zn** ($C_{12}H_{19.5}O_{18.75}SmZn_{1.5}$): C, 20.24; H, 2.76. Found: C, 20.49; H, 2.61.

Crystal Structure Determination. Diffraction intensities for **Sm−Co** and **Sm−Zn** were collected on a computer-controlled Bruker SMART 1000 CCD diffractometer equipped with graphite-monochromated Mo Kα radiation with radiation wavelength 0.710 73 Å by using the ω-scan technique. Lorentz polarization and absorption corrections were applied. The structures were solved by direct methods and refined with the full-matrix least-squares technique using the SHELXS-97 and SHELXL-97 programs.[10,11] Anisotropic thermal parameters were assigned to all non-hydrogen atoms. The hydrogen atoms were set in calculated positions and refined as riding atoms with a common fixed isotropic thermal parameter. Analytical expressions of neutral-atom scattering factors were employed, and anomalous dispersion corrections were incorporated. The crystallographic data and selected bond lengths and angles for **Sm−Co** and **Sm−Zn** are listed in Tables 1 and 2,

(8) (a) Zhao, B.; Gao, H.-L.; Chen, X.-Y.; Cheng, P.; Shi, W.; Liao, D.-Z.; Yan, S.-P.; Jiang, Z. H. *Chem.—Eur. J.* **2006**, *12*, 149. (b) Zhao, B.; Cheng, P.; Cheng, C.; Shi, W.; Liao, D.-Z.; Yan, S.-P.; Jiang, Z.-H. *J. Am. Chem. Soc.* **2004**, *126*, 3012. (c) Zhao, B.; Chen, X.-Y.; Cheng, P.; Liao, D.-Z.; Yan, S.-P.; Jiang, Z.-H. *J. Am. Chem. Soc.* **2004**, *126*, 15394.

(9) (a) Baggio, R.; Garland, M. T.; Moreno, Y.; Peòa, O.; Perec, M.; Spodine, E. *J. Chem. Soc., Dalton Trans.* **2000**, 2061. (b) Mao, J.-G.; Song, L.; Huang, X.-Y.; Huang, J.-S. *Polyhedron* **1997**, *16*, 963. (c) Baggio, R.; Garland, M. T.; Perec, M. *Inorg. Chim. Acta* **1998**, *281*, 18. (d) Liu, Q.-D.; Li, J.-R.; Gao, S.; Ma, B.-Q.; Liao, F.-H.; Zhou, Q.-Z.; Yu, K.-B. *Inorg. Chem. Commun.* **2001**, *4*, 301. (e) Barja, B.; Baggio, R.; Garland, M. T.; Aramendia, P. F.; Peòa, O.; Perec, M. *Inorg. Chim. Acta* **2003**, *346*, 187. (f) Grirrane, A.; Pastor, A.; Mealli, C.; Ienco, A.; Rosa, P.; Prado-Gotor, R.; Galindo, A. *Inorg. Chim. Acta* **2004**, *357*, 4215. (g) Jiang, C.; Wang, Z.-Y. *Polyhedron* **2003**, *22*, 2953. (h) Baggio, R.; Garland, M. T.; Perec, M. *Inorg. Chem.* **1997**, *36*, 950. (i) Baggio, R.; Garland, M. T.; Leyva, G.; Perec, M.; Polla, G. *Inorg. Chim. Acta* **2004**, *357*, 2185. (j) Nicola, C. D.; Galindo, A.; Hanna, J. V.; Marchetti, F.; Pettinari, C.; Pettinari, R.; Rivarola, E.; Skelton, B. W.; White, A. H. *Inorg. Chem.* **2005**, *44*, 3094. (k) Jianag, C.; Zhu, X.; Yu, Z.-P.; Wang, Z.-Y. *Inorg. Chem. Commun.* **2003**, *6*, 706. (l) Grirrane, A.; Pastor, A.; Álvarez, E.; Mealli, C.; Ienco, A.; Rosa, P.; Montilla, F.; Galindo, A. *Eur. J. Inorg. Chem.* **2004**, 707. (m) Rizzi, A. C.; Calvo, R.; Baggio, R.; Garland, M. T.; Peòa, O.; Perec, M. *Inorg. Chem.* **2002**, *41*, 5609. (n) Behrsing, T.; Deacon, G. B.; Forsyth, C. M.; Forsyth, M.; Skelton, B. W.; White, A. H. *Z. Anorg. Allg. Chem.* **2003**, *329*, 35. (o) Jiang, J.; Sarsfield, M. J.; Renshaw, J. C.; Livens, F. R.; Collison, D.; Charnock, J. M.; Helliwell, M.; Eccles, H. *Inorg. Chem.* **2002**, *41*, 2799. (p) Rao, L.; Garnov, A. Y.; Jiang, J.; Bernardo, P. D.; Zanonato, P.; Bismondo, A. *Inorg. Chem.* **2003**, *42*, 3685. (q) Mao, J.-G.; Huang, J.-S.; Ma, J.-F.; Ni, J.-Z. *Trans. Met. Chem.* **1997**, *22*, 277. (r) Mao, J.-G.; Song, L.; Huang, J.-S. *Jiegou Huaxue* **1997**, *16*, 228.

(10) Sheldrick, G. M. *SHELXS 97, Program for the Solution of Crystal Structures*; University of Göttingen: Göttingen, Germany, 1997.

(11) Sheldrick, G. M. *SHELXL 97, Program for the Refinement of Crystal Structures*; University of Göttingen: Göttingen, Germany, 1997.

Table 2. Selected Bond Lengths (Å) and Angles (deg) for **Sm−Co** and **Sm−Zn**[a]

		Sm−Co			
Co(2)−O(4)	2.081(6)	Sm(1)−O(3)	2.488(5)	Sm(1)−O(1)	2.425(4)
Co(1)−O(2)	2.109(4)	$O(1)^{\#1}$−Sm(1)−O(1)	78.94(15)	$O(2)^{\#7}$−Co(1)−O(2)	87.32(15)
$O(4)^{\#12}$−Co(2)−O(4)	90.000(1)	$O(1)^{\#1}$−Sm(1)−$O(1)^{\#3}$	146.86(19)	$O(1)^{\#1}$−Sm(1)−$O(1)^{\#5}$	86.5(2)
O(1)−Sm(1)−O(3)	63.69(9)	$O(2)^{\#6}$−Co(1)−$O(2)^{\#9}$	92.68(15)	$O(1)^{\#3}$−Sm(1)−O(1)	127.39(18)
O(1)−Sm(1)−$O(1)^{\#5}$	146.86(19)	$O(3)^{\#1}$−Sm(1)−O(3)	120.0	$O(2)^{\#6}$−Co(1)−O(2)	180.000(1)
$O(1)^{\#1}$−Sm(1)−O(3)	136.75(10)	$O(1)^{\#2}$−Sm(1)−O(3)	73.43(9)	$O(4)^{\#11}$−Co(2)−O(4)	180.0
		Sm−Zn			
Sm(1)−O(1)	2.436(5)	Sm(1)−$O(3)^{\#3}$	2.511(7)	ZnI1−O(2)	2.061(5)
Sm(1)−O(3)	2.512(6)	ZnI1−O(4)	2.148(7)	$O(1)^{\#3}$−Sm(1)−O(1)	79.34(19)
O(4)−ZnI1−$O(4)^{\#7}$	179.999(2)	$O(2)^{\#6}$−ZnI1−O(2)	91.2(4)	$O(1)^{\#1}$−Sm(1)−O(3)	136.83(12)
$O(1)^{\#4}$−Sm(1)−O(1)	125.6(2)	$O(2)^{\#7}$−ZnI1−O(2)	179.997(1)	$O(2)^{\#6}$−ZnI1−O(4)	87.0(2)
$O(1)^{\#1}$−Sm(1)−O(1)	148.4(2)	O(2)−ZnI1−O(4)	93.0(2)	$O(2)^{\#8}$−ZnI1−O(2)	88.8(4)
$O(3)^{\#2}$−Sm(1)−O(3)	119.999(1)	$O(1)^{\#5}$−Sm(1)−O(1)	86.3(2)	O(1)−Sm(1)−O(3)	62.79(11)
$O(1)^{\#3}$−Sm(1)−O(3)	74.21(12)	$O(3)^{\#3}$−Sm(1)−O(3)	120.0		

[a] Symmetry transformations used to generate equivalent atoms are as follows. **Sm−Co**: #1, $x, -y + 3/4, -z + 3/4$; #2, $-x, y + 3/4, z - 3/4$; #3, $x + 3/4, -y, z - 3/4$; #4, $-x + 3/4, y, -z + 3/4$; #5, $-x, -y, -z + 3/2$; #6, $-x, -y, -z + 2$; #7, $x, y + 1, z - 1$; #8, $-x + 1, -y, -z + 1$; #9, $x + 1, y, z - 1$; #10, $-x, -y + 1, -z + 1$; #11, $-x + 5/4, -y + 5/4, z$; #12, $-x + 3/4, -y + 5/4, z + 1/2$; #13, $x, y - 1/2, z + 1/2$; #14, $-x + 5/4, -y + 3/4, z + 1/2$; #15, $x - 1/2, y, z + 1/2$. **Sm−Zn**: #1, $x, x - y + 1, -z + 1/2$; #2, $-x + 1, -x + y, z$; #3, $x - y + 1, -y + 1, z$; #4, $-x + 1, -y + 1, -z + 1/2$; #5, $-x + y, y, -z + 1/2$; #6, $-x + 1, -y + 2, z$; #7, $-x + 1, -y + 2, -z$; #8, $x, y, -z$.

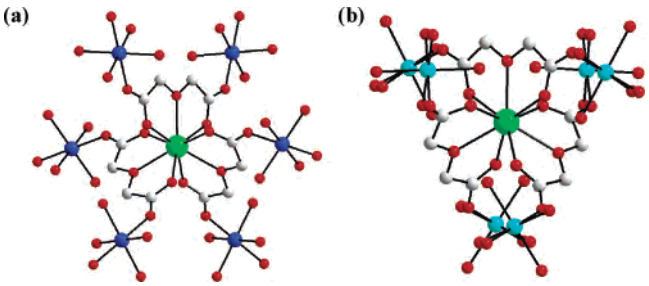

Figure 1. Coordination units in the crystal structures of **Sm−Co** (a) and **Sm−Zn** (b). Key: red, O; gray, C; blue, Co; cyan, Zn; green, Sm; hydrogen atoms omitted for clarity.

respectively. CCDC Nos. 617289 (**Sm−Co**) and 617129 (**Sm−Zn**) contain the supporting crystallographic data for this paper. These data can be obtained free of charge via www.ccdc.can.ac.uk/conts/retrieving.html.

Results and Discussion

Structural Analysis of Sm−Co and Sm−Zn. X-ray structure analyses reveal that the 3D coordination network of dark red cubic **Sm−Co** crystallizes in the cubic crystal system, space group $Fd\bar{3}c$, and contains two distinct types of building blocks, $Sm(L)_3$ and CoO_6. The octahedron coordination geometry around Co(II) center comprises six O atoms from the carboxyl groups of six L ligands. Each ligand chelates to one Sm atom and bonds to two Co atoms in an *anti-anti* configuration (Figure 1). Therefore, each Sm(III) center has six Co(II) ions as the nearest metal center and each Co(II) center has six Sm(III) ions in its vicinity, which is consistent with the Co/Sm molar ratio (1:1). Sm and Co atoms are arrayed alternatively and connected by O−C−O bridges to form a $Sm_4Co_4(COO)_{12}$ cubic octahedral cage as the secondary building unit (SBU), which was further assembled into a primitive cubic network with high symmetry (Figure 2). $[Co(H_2O)_6]^{2+}$ and $(H_2O)_6$ exist as guests in **Sm−Co**, and the distance between Co atoms in the side is 12.99 Å. The hydrogen bonds are linear, and the separations between of O1···O2 and O2···O2A are 3.22 and 2.40 Å, respectively. As a result, a cubic supramolecular SBU with Co2−O···O···O···O−Co2 as sides is

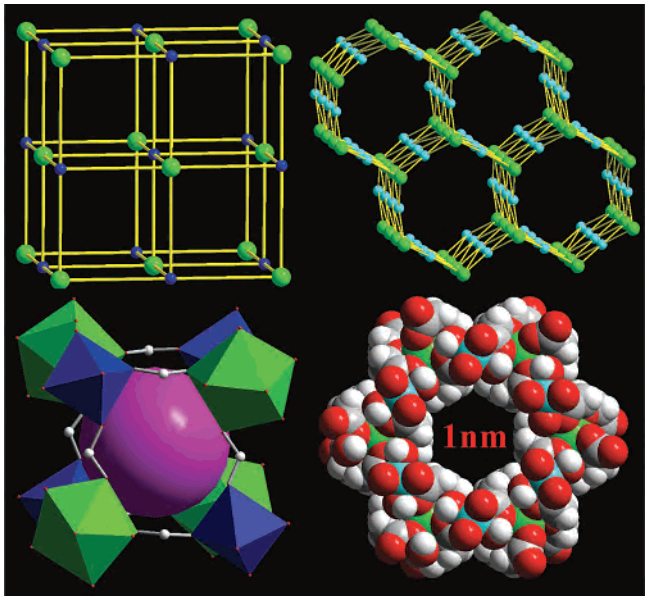

Figure 2. Topological NaCl network and a cubic building block in **Sm−Co** (upper and lower left) and perspective view of nanotubes and space-filling diagram of a hexagonal aperture with diagonals of 1 nm in **Sm−Zn** (upper and lower right). Key: red, O; gray, C; blue, Co; cyan, Zn; green, Sm; white, H; yellow line, bridged carboxylate group; purple sphere, the void inside the cuboctahedral cage.

formed and an interesting 2-fold interpenetrating 3D hydrogen-bonding supramolecular network has been constructed (Figure 3).

$[Co(H_2O)_6]^{2+}$ act as the thermodynamically stable species, required to balance the two negative charges of $[Sm_2(L)_6Co_2]^{2-}$ in **Sm−Co**, while the deprotonation of a water molecule from $[Zn(H_2O)_6]^{2+}$ resulted in the collapse of the octahedral structure and all the hydrolysis species had a coordination number of less than 6.[12] Therefore, NaCl network may not emerge in **Sm−Zn**. Such consideration is demonstrated by the crystal structure of coordination polymer $\{[Sm_2(L)_6Zn_3(H_2O)_6]\cdot 1.5H_2O\}_n$ (**Sm−Zn**). **Sm−Zn** crystallizes in the hexagonal crystal system, space group *P*6/*mcc*. Each L adopts a *syn−syn* configuration to link two Zn^{2+} ions (Figure 1).

(12) Zhu, M. Q.; Pan, G. *J. Phys. Chem. A* **2005**, *109*, 7648.

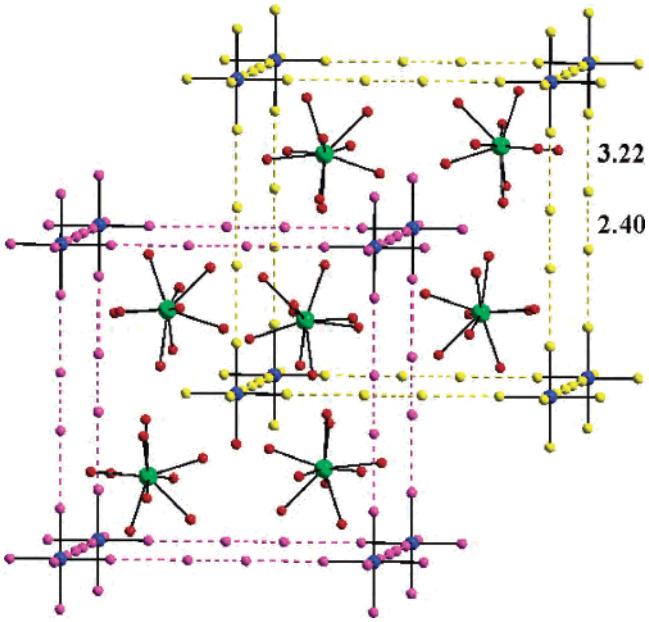

Figure 3. 2-fold interpenetrating 3D supramolecular network in **Sm−Co**. Key: blue, Co; green, Sm; red, O atom coordinated with Sm; yellow and purple, O atom in each side of cubic supramolecular network; dotted line, hydrogen bond; black line, coordinated bond; C and H atoms omitted for clarity.

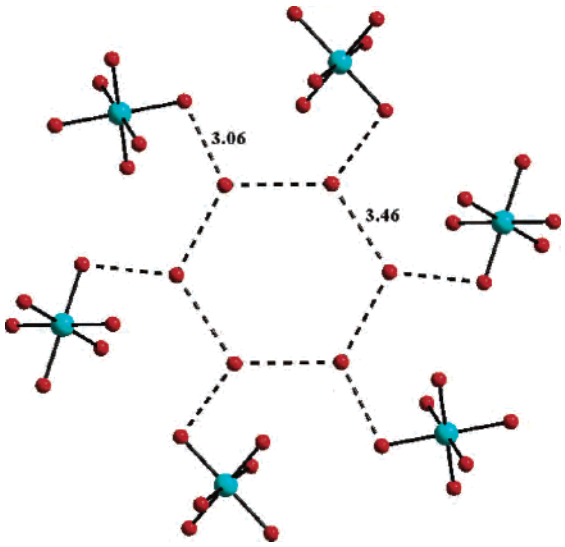

Figure 4. Distances between the adjacent water molecules in the nanotube and hydrogen bonds between the guest and coordinated water molecules in **Sm−Zn**. Key: cyan, Zn; red, O; black solid line, coordinated bond.

Carboxylate groups bridge adjacent Sm and Zn atoms to create two kinds of metallocycles, $Sm_2(COO)_4Zn_2$ and $Sm_6(COO)_{12}Zn_6$, to be further assembled into a highly ordered 3D nanotubular structure (Figure 2). In **Sm−Zn**, six discrete guest water molecules are rigidly coplanar and form a hexagon with equal edge lengths of 3.46 Å. Such water hexamers are stabilized by hydrogen bonds with the coordinated water molecules of Zn atoms (Figure 4). The effective opening of **Sm−Zn** by taking into account the van der Waals volume of the atoms can be described as a hexagonal section with sides of about 5 Å and diagonals of 10 Å. The potential free volume accessible for water molecules determined by PLATON calculations is about 34% of void/unit volume.[13] The pore in **Sm−Zn** is the largest one among the heterometallic coordination polymers reported to date.

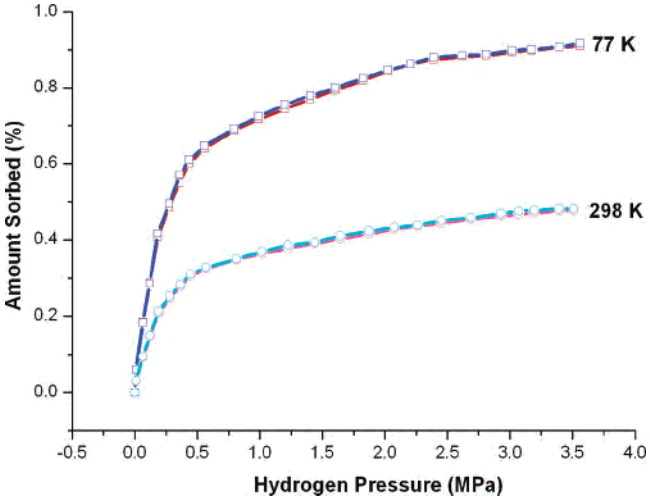

Figure 5. Reversible hydrogen adsorption isotherms of **Sm−Zn** activated at 170 °C.

It is noted that although the Sm/M/L ratio (2:3:6) and the synthesis conditions are similar, the structures of **Sm−Co** and **Sm−Zn** comprise different kinds of heterometallic 3D networks with different topologies. These two distinct ligand configurations, a major driving force to produce two types of products, exist in the reaction solution and result in different assembly directions of Sm^{3+} and transition metal ions.

Adsorption Property of Sm−Zn. Because $[Co(H_2O)_6]^{2+}$ guests occupy the channel of **Sm−Co**, **Sm−Zn** was allowed to undergo to hydrogen adsorption, which represents the first investigation of gas adsorption in heterometallic microporous coordination polymer. Microcrystals of **Sm−Zn** outgassed at 170 °C overnight shows a large weight loss of 9.8%, which corresponds to expectation. The hydrogen uptake, measured at 298 and 77 K, shows a very fast adsorption process, and thermodynamic equilibrium is reached in a few seconds, as expected for physisorption. At room temperature, the hydrogen gas isotherm curve increases with pressure up to 0.54 wt % under approximately 3.5 MPa. Under much lower pressure done with **Sm−Zn** than that for MOF-5 and $Cu_3(btc)_2$ (65 bar),[14] they exhibit smaller hydrogen uptake (0.28 and 0.35 wt %, respectively). At 77 K, hydrogen adsorption is significant at low pressure with a maximum capacity of 1.19 wt % under 3.4 MPa (Figure 5), which is relatively low with comparison to that of $Cu_3(TATB)_2(H_2O)_3$ (1.9 wt %).[4b] In the copper complex, the resulting triangular channels are connected by windows as small as about 5 Å, almost the same distance of each side of a hexagonal section in **Sm−Zn**. The carboxylate functionality of TATB leads directly to the formation of the well-understood tetracarboxylate paddlewheel SBU occupying each vertex of the cuboctahedral cage. This provides more tunable and larger

(13) Spek, A. L. *PLATON, A Multipurpose Crystallographic Tool*; University of Utrecht: Utrecht, The Netherlands, 2001.
(14) Panella, B.; Hirscher, M.; Pütter, H.; Müller, U. *Adv. Funct. Mater.* **2006**, *16*, 520.

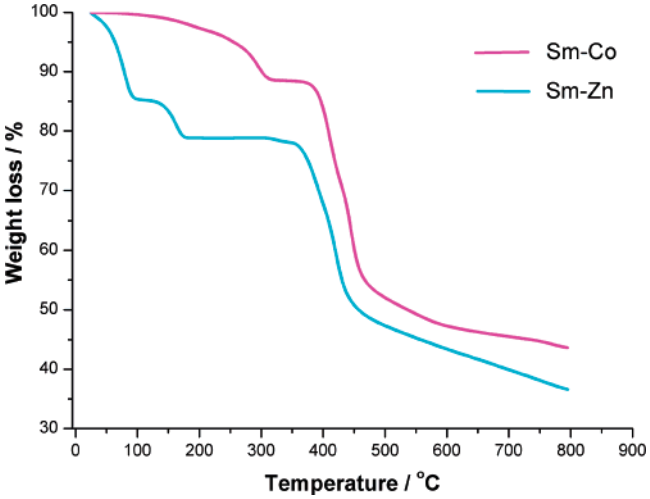

Figure 6. TGA plots of **Sm−Co** and **Sm−Zn**.

cavities with the average diameter of the void inside the cuboctahedron being 30.3 Å, which is much larger than that in **Sm−Zn**.

The shape of the isotherm reveals type-I behavior, which is typical for microporous materials, indicating that H_2 is truly adsorbed in the pores and the pore size limits the adsorption to one or a few molecular layers. The adsorption isotherm is independent of the number of adsorption cycles, which proves that the hydrogen uptake of **Sm−Zn** is completely reversible. The surface area and micropore volume, estimated by applying the BET and Dubinin−Raduskhvich equations, are 718.8 m^2/ g and 0.31 cm^3/g, respectively, which are higher than those in CUK-2 (420 m^2/g, 0.17 cm^3/g) but significantly smaller than the highest surface area (5500 m^2/g) and the largest total pore volume (1.9 cm^3/g) reported in porous materials.[3a] Apart from high specific surface area, another important factor for hydrogen adsorption is the presence of strong adsorption sites like the unsaturated metal sites of Zn^{2+} ions in **Sm−Zn**.

Thermal Stability of Sm−Co and Sm−Zn. The TGA curve (Figure 6) shows that the guest and coordinated water molecules are removed in the temperature range 25−300 °C for **Sm−Co** and 25−170 °C for **Sm−Zn**, indicating strong hydrogen-bonding interactions exist in **Sm−Co**. At 370 °C, the coordination networks of both **Sm−Co** and **Sm−Zn** begin to decompose. Noticeable diffraction intensity variations in the PXRD patterns of **Sm−Zn** are observed between 90 and 150 °C, accompanied with slight position shifts of

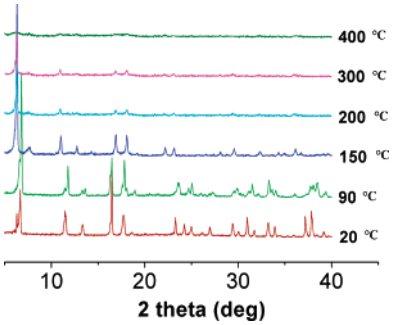

Figure 7. X-ray powder diffraction patterns of **Sm−Zn** under air from 20 to 400 °C.

the Bragg peaks (Figure 7). This is ascribed to small structural rearrangements consecutive to the departure of coordination water molecules.[15] Above 400 °C, the long-range order disappears and there comes into being an amorphous phase.

Conclusion

In summary, two types of 3D heterometallic complexes with high symmetry based on oxydiacetic acid were obtained. **Sm−Co** represents a kind of anionic porous MOF, which is rare in 3D zeolite-like coordination polymers and contains interesting 2-fold interpenetrating 3D hydrogen-bonding supramolecular networks. **Sm−Zn** represents the largest porous material among heterometallic coordination polymers and the first example used to investigate hydrogen adsorption. **Sm−Zn** possesses hydrogen storage capacity of up to 1.19 wt % at 77 K and 0.54 wt % at 298 K, respectively. Further work will focus on the syntheses of other heterometallic complexes with higher affinities for hydrogen gas.

Acknowledgment. This work was supported by the National Natural Science Foundation of China (Grants 20631030 and 20425103), the NSF of Tianjin (Grant 06YFJZJC009000), the State Key Project of Fundamental Research of MOST (Grant 2005CCA01200), and MOE (Grant 20060055039) of China.

Supporting Information Available: X-ray crystallographic files (CIF) for **Sm−Co** and **Sm−Zn**. This material is available free of charge via the Internet at http://pubs.acs.org.

IC070097R

(15) Chen, X.-Y.; Zhao, B.; Shi, W.; Xia, J.; Cheng, P.; Liao, D.-Z.; Yan, S.-P.; Jiang, Z.-H. *Chem. Mater.* **2005**, *17*, 2866.